Minimally Invasive Local-Skull Electrophysiological Modification With Piezoelectric Drill

Yike Sun, *Graduate Student Member, IEEE*, Anruo Shen, Jingnan Sun, Chenlin Du, Xiaogang Chen, *Member, IEEE*, Yijun Wang, *Member, IEEE*, Weihua Pei, *Member, IEEE*, and Xiaorong Gao, *Member, IEEE*

***Abstract*— The research on non-invasive BCI is nowadays hitting the bottleneck due to the humble quality of scalp EEG signals. Whereas invasive solutions that offer higher signal quality in contrast are suffocated in their spreading because of the potential surgical complication and health risks caused by electrode implantation. Therefore, it puts forward a necessity to explore a scheme that could both collect high-quality EEG signals and guarantee high-level operation safety.This study proposed a Minimally Invasive Local-skull Electrophysiological Modification method to improve scalp EEG signals qualities at specific brain regions. Six eight-month-old SD rats were used for in vivo verification experiment. A hole with a diameter of about 500 micrometers was drilled in the skull above the visual cortex of rats. Significant changes in rsEEG and SSVEP signals before and after modification were observed. After modification, the skull impedance of rats decreases by about 84 %, the average maximum bandwidth of rsEEG increase by 57 %, and the broadband SNR of SSVEP is increased by 5.13 dB. The time of piezoelectric drilling operation is strictly controlled under 30 seconds for each rat to prevent possible brain damage from overheating. Compared with traditional invasive procedures such as ECoG, Minimally Invasive Local-skull Electrophysiological Modification operation time is shorter and no electrode implantation is needed while it remarkably boosts the scalp EEG signal quality. This technical solution has the potential to replace the use of ECoG in certain application scenarios and further invigorate studies in the field of scalp EEG in the future.**

***Index Terms*— Brain-computer interface, skull modification, minimally invasive, SSVEP, EEG.**

Manuscript received 4 May 2022; revised 29 June 2022; accepted 17 July 2022. Date of publication 20 July 2022; date of current version 26 July 2022. This work was supported in part by the Key Research and Development Program of Ningxia Hui Autonomous Region under Grant 2022CMG02026, in part by the Key-Area Research and Development Program of Guangdong Province under Grant 2018B030339001, and in part by the Beijing Science and Technology Plan under Grant Z201100004420015. *(Corresponding author: Xiaorong Gao.)*

Yike Sun, Anruo Shen, Jingnan Sun, Chenlin Du, and Xiaorong Gao are with the Department of Biomedical Engineering, Tsinghua University, Beijing 100084, China (e-mail: sun.yk.bci@outlook.com; gxr-dea@tsinghua.edu.cn).

Xiaogang Chen is with the Institute of Biomedical Engineering, Chinese Academy of Medical Sciences and Peking Union Medical College, Tianjin 300192, China.

Yijun Wang and Weihua Pei are with the Institute of Semiconductors, Chinese Academy of Sciences, Beijing 100083, China.

Digital Object Identifier 10.1109/TNSRE.2022.3192543

I. Introduction

BRAIN-COMPUTER interface (BCI) technology is one of the research hotspots in neural engineering [1], [2]. The difference in signal sources can be divided into two categories: non-invasive BCI and invasive BCI [3], [4]. The non-invasive BCI that based on Electroencephalogram (EEG) has attracted wide attention from researchers and industries because of its undeniable safety and convenience [5], [6]. However, due to the relatively low quality of EEG signals, its limitations in real practices are also still large [7], [8]. In fact, the quality of signals obtained via invasive BCI such as Electrocorticography (ECoG) significantly outperforms EEG in the signal quality [9]. According to the study by Benjamin *et al.* in 2018, the Steady-State Visual Evoked Potentials (SSVEP) recorded by ECoG is about 7 dB higher than that recorded by EEG [10]. However, its drawbacks such as health problems resulting from electrode implantation [11], high risk of craniotomy [12], and the attendant ethical problems [13], [14] make it nearly impossible to be widely promoted among healthy people. Therefore, exploring a signal acquisition method to balance between moderate signal quality and surgical risk is an emerging problem to solve in the field of BCI research and development.

There are multiple different tissues lying between cerebral cortex and EEG electrodes on the scalp, where the skull's electrical resistivity is prominently the highest among them, making it the largest blockage of EEG signals [15]. There since have been many studies on the obstruction effect of skull over EEG signals. Rush *et al.* carried out an experiment using a half-dry skull and found that the conductivity ratio of the penetrating fluid to the immersed skull was 80 [16], so they believed that the electrical resistivity ratio of the scalp to the skull should also be 80 [17]. More recently, some scholars have concluded from in vivo and in vitro bidirectional tests that the electrical resistance ratio of the scalp to skull should be around 15, assuming that the whole skull is homogeneous.[18], [19]. However, human brain is sophisticatedly heterogeneous, composed of eight bones with the thickness of each being slightly different, and the suture structure of it also varies from other parts [20]. Some scholars have discovered that the EEG signals obtained on some relatively thin bones and sutures are largely different from others [21]. Furthermore, cranial damage can also cause signal

This work is licensed under a Creative Commons Attribution 4.0 License. For more information, see https://creativecommons.org/licenses/by/4.0/

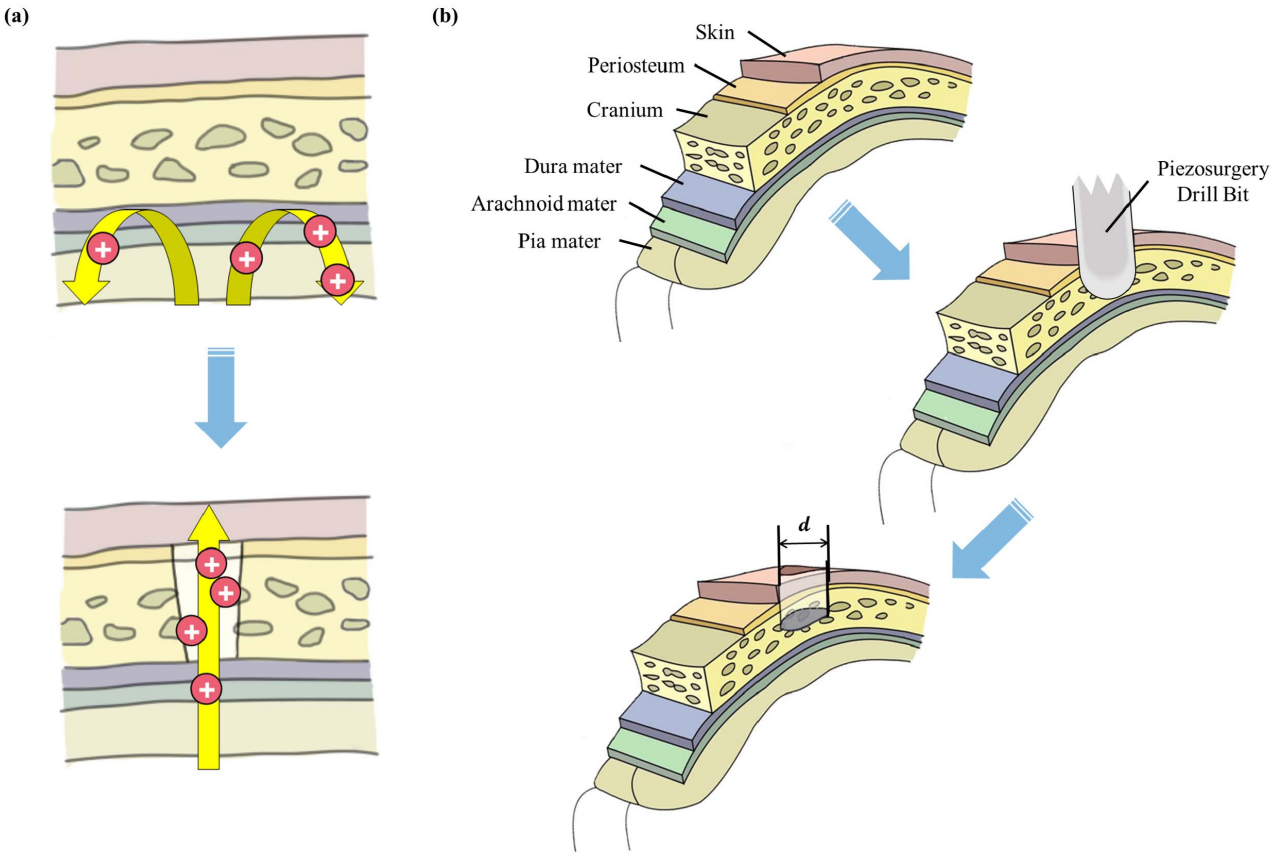

Fig. 1. (a) Bio current flow diagram before and after skull reconstruction. (b) The schematic diagram of the MILEM process. We use a piezoelectric drill to smash bone tissue subcutaneously via high-frequency physical resonance.

mutations. Evidences show that the amplitude of evoked potential EEG signals collected at the site of skull damage increased significantly [22]–[24]. Kendel *et al.* compared the EEG signals at the defect site and its symmetrical position of 30 patients with skull defect and found that the amplitude of signal amplitude at the defect was five times higher than that at the same area on the opposite side [25]. Cobb *et al.* studied 33 people with a skull fracture and found that the alpha frequency band energy was significantly improved [26]. The above results demonstrate that it is feasible to improve the signal quality of specific brain regions by changing local electrical conductivity through small-scale surgery.

Current BCI technology, commonly utilizing paradigms such as SSVEP [27], motor imagery [28], and P300 [29], relies heavily on the decoding of specific signals in particular brain regions [5]. Therefore, it is consistently looking for better EEG signals for better application effect. Given that previous studies have verified that signal amplitude can be changed through local skull conductivity transformations [22]–[26], we proposed a local skull electrophysiological modification (MILEM) scheme to help restore signal quality. The bone tissue covering task-related brain regions of the specific BCI paradigm is to be perforated by a piezoelectric drill to overcome signal decay across the skull obstacle and thus to enable the scalp electrode to obtain high-quality EEG signals.

II. Methods

A. Skull Electrophysiological Modification

The skull's hindrance to EEG signals is enormous [15], which can block ion flow and thereby block the propagation of EEG signals from the cortex to the scalp [30]. But once the skull hole is penetrated, allowing the tissue fluid to naturally fill in the hole, it would open a pathway for ion current to travel though, leading to a significant increase in the signal amplitude detected on the scalp, as shown in Figure 1 (a).

Figure 1 (b) demonstrates the process of the MILEM. For the start, the drill bit is directly inserted into the subcutaneous layer and positioned right on the skull. After stabilization, ultrasound is enabled by the transducer to pierce the skull. Based on Salem *et al.* ' s 2019 study indicating that opening a centimeter-level hole in the patient's skull does not have significant effect on physiological indicators such as intracranial pressure [31], the pore diameter was set about 500 micrometers in this operation protocol.

Piezoelectric technology is chosen to generate high-intensity focused ultrasound in aim to penetrate the bone tissue. Piezoelectric surgical devices are often used in clinical fields such as dental surgery [32], [33]. Given the fact that human tissues have different resonance frequencies, by outputting adequate frequency, the piezoelectric technology can achieve the effect of penetrating bone tissue without injuring soft

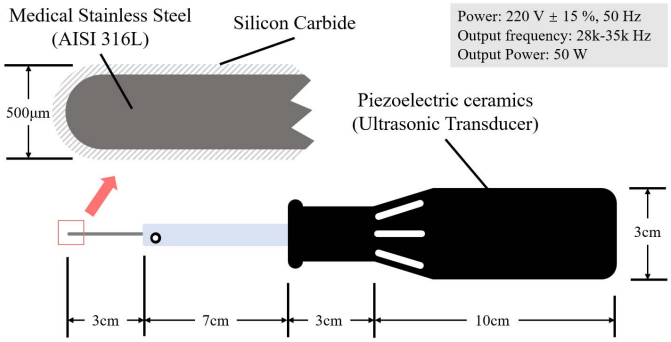

Fig. 2. Diagram of the piezoelectric drill. The drill is composed of a stainless-steel core and a silicon carbide layer on the surface. The back end of the drill is connected with an ultrasonic transducer made of piezoelectric ceramics. Its output ultrasonic frequency range is 28-35 kHz, and the output power is 50W.

tissue [34], [35]. However, according to Kotrikov *et al.*, although piezosurgery can effectively protect the dura mater during craniotomy, its cutting time is more than twice that of traditional technology which might account for the reason why it has not been widely used nowadays [36]. In our study, in regard of this issue, cutting time is strictly limited within 30s to avoid collateral damage. To meet demand of such higher operating efficiency, a piezoelectric surgical drill is specially designed and used. The drill bit is shown in Figure 2.

B. Steady-State Visual Evoked Potentials Paradigm

Steady-State Visual Evoked Potentials (SSVEP) is a standard visual evoked potential [37] found in various mammalian groups [38], [39]. Due to its unique frequency-following characteristics and the strong energy that is measurable for EEG, this paradigm is greatly employed in BCI research [5], [40]. In our experiment, SSVEP is used as a signal indicator to compare the EEG signal quality before and after MILEM. As shown in Figure 3 (a), rats are made to stare at the stimulus screen in a room where the ambient light is masked. A single SSVEP test trial consists of a 10s full-screen SSVEP stimulus target and two 2s preparation time before and after the stimulation (Fig. 3 (b)). We adopted sinusoidal stimulation and set its frequency above 10 Hz to avoid ECG interference (the heart rate of rats was between 370 and 580 beats/min, i. e., about 9 Hz). Different frequencies is designed with an increasing interval of 2 Hz (11, 13, 15, 17, 19 Hz). There were five trials for each stimulus frequency. The sequence is randomized by computer programs.

C. Design of Experiment

In order to verify the effectiveness of MILEM, we conduct the before-after study through in vivo experiments on rat models to examine the change of impedance and EEG values. Six 8-month-old SD rats were used (Female: Rat 01, Rat 02, Rat 03; Male: Rat 04, Rat 05, Rat 06). The lead position of the EEG is shown in Figure 4 (a). We use the ear of the rat as the Ground lead of the EEG while placing Ref lead above the junction between neck and skull to offset the ECG interference. In the experiment, MILEM was performed on the skull

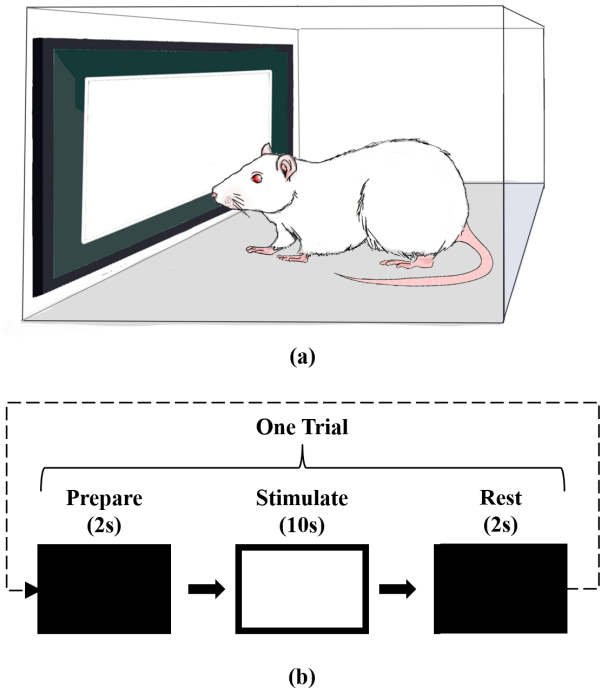

Fig. 3. (a) A schematic diagram of the SSVEP experimental environment. Fix the head of the rat in front of the stimulus screen in the dark. (b) Single-trial schematic diagram of SSVEP experiment. Each trial consists of a two-second preparation environment, a ten-second stimulus, and a two-second rest. In preparation and rest, the stimulus screen does not output any images.

above the visual area, and the modification point is shown in Figure 4 (b). We respectively recorded the impedance values from inner ear of the rats to the skin above the modified point and their electrophysiology data (rsEEG and SSVEP). The experimental diagram is shown in Figure 4 (c). Since EEG signals have this feature of constantly-changing, meaning its value varies dramatically across days and other time scales [41], we measure all the EEG data under continuous anesthesia after surgery to avoid unfixable differences caused by time factors. Besides, to investigate the healing condition of holes, we euthanized three rats and took out their skulls at different times after the surgery for closer observation. The above experimental scheme has been reviewed by the Laboratory Animal Ethics Committee of Tsinghua University.

D. Data Record

1) Electric Impedance Measure by LCR Digital Bridge: We measure the impedance of rats' skull using LCR digital bridge (Agilent HP 4284) and its matching fixture (Agilent 16089A Kelvin Clip Lead Set). A precision LCR bridge with a frequency range from 20 Hz to 1 MHz. The frequency range is 5Hz to 100kHz, and DC Bias is -42v to 42v.

2) EEG Record: In EEG recordings, we used a 16-lead amplifier produced by Neuracle with the sampling rate of 1000Hz. In order to simulate the human body, AgCl EEG electrodes produced by Neuroscan were used. SSVEP stimulation program was programmed using Psychophysics Toolbox Version 3 of Matlab 2020 [42]. The stimulus screen uses

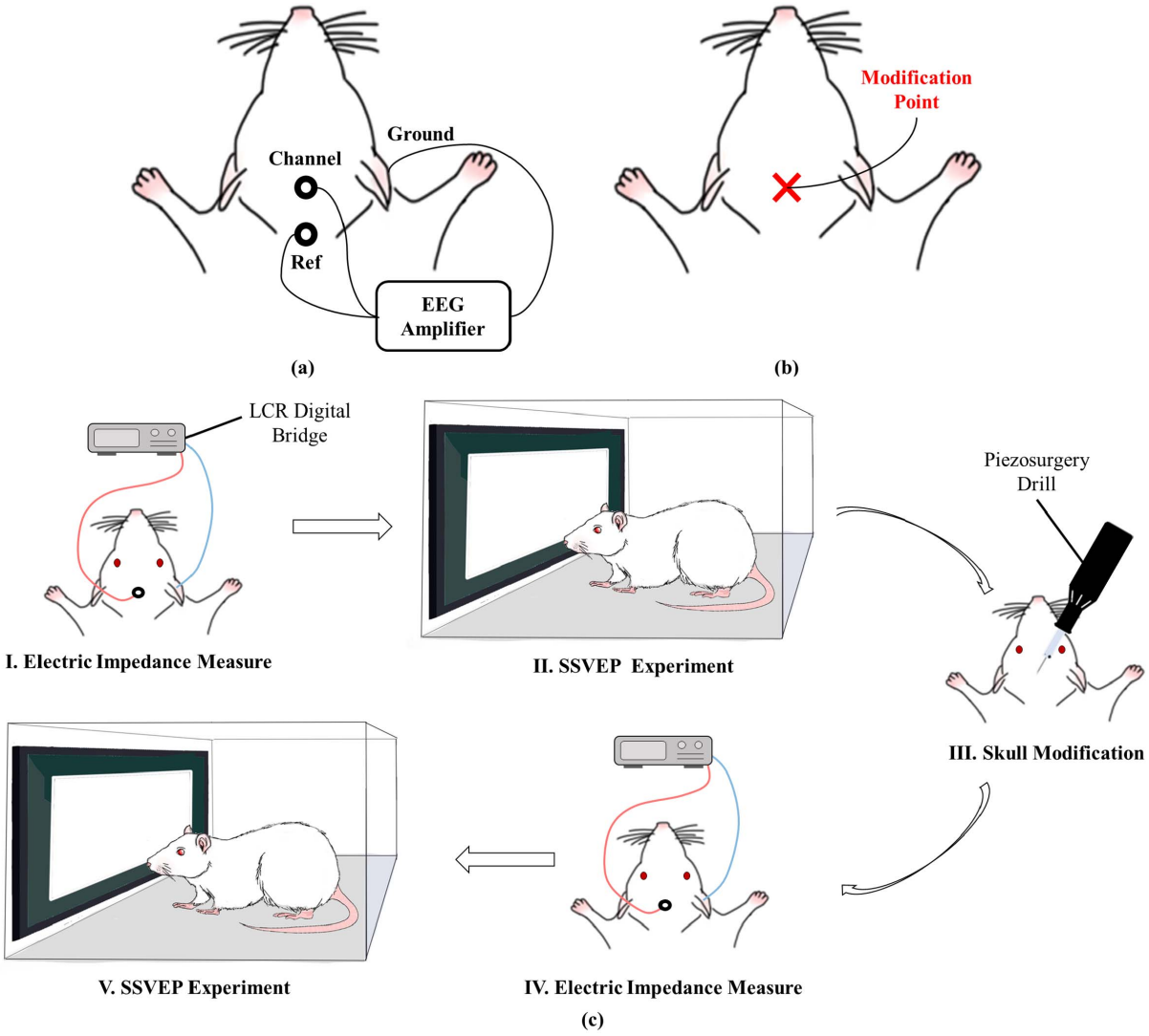

Fig. 4. (a) The experimental EEG leads position diagram. The Channel lead covers the skull reconstruction point above the visual area according to the SSVEP paradigm. Ref lead is located at the rat skull and neck junction to offset ECG signals. The Ground lead is in the rat ear. (b) Skull modification point diagram. (c) Experimental process diagram. After the experiment started, we first used the LCR digital bridge to measure the impedance value of the ear of rats to the modification point. Then SSVEP experiment was performed, and EEG data were recorded. Then we completed the minimally invasive skull local electrophysiological modification and repeat previous impedance measurement and EEG collection.

a VG278HE LCD produced by ASUS with a resolution of 1920×1080. Before each experiment, we confirmed the time length of each frame of the stimulus screen to ensure the stability of visual stimuli.

E. EEG Data Process

1) Preprocess: All the experimental data recorded by EEG were extracted according to the event generated by the stimulus program. Then we use the IIR elliptic filter with a cut-off frequency of 5Hz to 100Hz to process, and then use the comb filter to do notch processing. Finally, we downsampled the filtered data from 1000Hz to 250Hz.

2) SNR: The broadband signal-to-noise ratio [43] is a standard indicator of SSVEP performance. The SSVEP response and its harmonic frequency components are regarded as signals, and the other frequency components are regarded as noise. Its mathematical expression is as follows.

$$SNR = 10 * \log_{10}\left[\frac{N\left(f_{\text{ssvep}}\right)}{\sum_{f=f_l}^{f_h} N(f) - N\left(f_{\text{ssvep}}\right)}\right] \quad (1)$$

N(f) represents the spectrum energy in f. f_l is the lower limit of frequency band and f_h is the higher limit of frequency band, which are 10 Hz and 20 Hz for this research. f_{ssvep} is the frequency of stimulus target.

3) Highest Effective Frequency: In EEG research, the highest effective frequency is still unknown. In clinical studies, it is generally believed that the available frequency band of EEG is between 0.5 Hz and 50 Hz [44]. This study referred to some articles on intracranial electrodes [45], [46] and proposed a method to measure the highest effective frequency. In practice, researchers generally believe that EEG signals above 100Hz are meaningless, so we use the 85Hz to 95Hz

frequency band as a noise floor because it is the maximum 10Hz bandwidth below 100Hz that is not close to any power frequency we are interested in. In this study, the Welch method was used to calculate the power of each frequency component of rsEEG. Take random power array of 10Hz frequency band and conduct paired t-test with that of the noise floor. If the p-value is less than 0.01, we consider that the band contains valid information. Starting from 0Hz, we traverse all 10Hz frequency bands in turn until the p-value is higher than 0.01, then we take the starting frequency of this band as the highest effective frequency.

III. Results

We measured the electrical impedance from 20Hz to 1000Hz using LCR digital bridge. The results are shown in Figure 5 (a). The electrical impedance value after modification ($M = 3.72k\Omega$, $SD = 0.27$) was significantly lower than that before modification ($M = 23.1k\Omega$, $SD = 5.02$), $t(5) = 8.67$, $p = .00034 < .05$. The average electrical impedance decreased by about 84 %. Figure 5 (b) is the scatter plot of the electric impedance value of each rat before and after the modification when the measurement frequency is 1000Hz. We can see from the figure that the scatters are concentrated in the lower right corner, denoting that the conclusion of impedance decrease is sound.

Figure 5 (c) is the frequency spectrum of EEG signals recorded by Rat 02 at 13 Hz stimulation, from which we can see SSVEP signals that are not obvious before modification become distinct after MILEM. Furthermore, this modification also helps bring suppression to the background noise, thus further elevating the SNR value. Fig. 5 (d) shows the broadband signal-to-noise ratio of SSVEP in each rat before and after modification. The SNR of SSVEP after modification ($M = -20.08$ dB, $SD = 1.99$) is significantly higher than that before modification ($M = -25.22$ dB, $SD = 1.81$), $t(10) = 4.67$, $p = .0009 < .05$. The average SNR increased by about 5.13 dB. SNR results for each rat and each stimulate frequency are shown in Fig. 5 (e). It can be seen that the SSVEP signal recorded from the electrodes on the scalp of each rat was significantly enhanced after MILEM.

We also used the Welch method to calculate the power spectral density (PSD) of rsEEG before and after MILEM, the result of which is shown in Figure 6 (a). From the yellow part, which is increased value by MILEM, it can be clearly seen that the improvements of low-frequency components are more significant. Figure 6 (c) shows the highest effective frequency of six rats before and after the modification, and the dotted line represents the highest effective frequency position. The highest effective frequency ($M = 75.25$ Hz, $SD = 3.99$) after modification was 57 % higher than that before modification ($M = 47.84$ Hz, $SD = 14.35$), $t(5) = 5.83$, $p = .0021 < .05$. The relevant results can be found in Figure 6 (b). The survival rate of 6 rats was 100 % three months after the operation, and no obvious infection was found.

Three SD male rats were separately euthanatized immediately, one week, and three months after surgery to explore the skull healing process. Figure 7 (a) shows the photo of the skull hole, where I. is a timely post-operative hole photo, II. shows the hole a week later, and III. shows the hole three-month later. With the passage of time, the holes' size remains almost the same, implying that the holes MILEM created have no obvious healing tendency.

The whole procedure was short for it doesn't involve invasive operations. Figure 7 (b) shows the electrical impedance results recorded by the LCR bridge at different times after MILEM at 1000Hz measurement frequency. At the same time, Figure 7 (c) shows the average time we recorded in the experiment. Neither the value of electrical impedance nor the diameter of the skull holes changed significantly with time after MILEM. For each rat, the skull modification operation was completed within 30 s and rats could move normally just 30 mins later after anesthesia stops.

IV. Discussion

A. Effect of Anesthesia on EEG

In the process of this study, how to record animal scalp EEG is a big challenge. Animals normally would not cooperate with experimental procedures in its full wakefulness and their moving around greatly polluted EEG signals we are interested in with Electromyogram (EMG), which is hard to purify through later-stage processing and eventually mess-up with the whole data collected. Therefore, anesthesia is essential for animal EEG experiments. We acquired a critical anesthetic concentration that equilibrate between low EMG and decent EEG through a priori experiment, along with determining the optimal position for electrode placement. However, with all the precautionary efforts, the SNR of the SSVEP signal obtained are still significantly lower than that of a human in the awake state [47] informing that anesthesia still has an inevitable influence on nerve activities. For the whole field of animal EEG research, it is still necessary to explore ways to shun the effect of anesthesia as much as possible.

B. SSVEP Signal Not Obvious Before Modification

In practice, we found that if the SNR is lower than −20dB, it is almost impossible to see the peak of SSVEP in the spectrum. Figure 5 (e) shows that it is difficult to see an apparent SSVEP signal in the rat EEG before modification. Nevertheless, after MILEM, SSVEP signals became obvious. With a more vivid saying, the extent of change brought by MILEM is more like 'from none to existence' than 'from less to more'. However, this does not mean there is no SSVEP signal in the rat brain before modification. Through literature review, we found a few cases that have successfully recorded SSVEP signals using intracranial electrodes [38], showing that SSVEP does exist in a rat's brain under anesthesia. Thus, we believe the reason why we could barely detect SSVEP signals on the scalp before MILEM is because of its power being too weak to break through the skull barrier.

C. Potential Applications

Although the initial aim of our study is to boost the EEG signal so as to enhance the usability of noninvasive BCI,

Fig. 5. (a) Shows the change of electric impedance from the ear to the modification point before and after the modification at different test frequencies, p=.00034. (b) shows the scatter plot of the electric impedance of each rat before and after modification when the test frequency is 1000Hz. (c) is the spectrum of EEG signal recorded by Rat 02 at the stimulation frequency of 13 Hz, and the amplitude has been normalized for facilitate comparison. (d) is the average SSVEP broadband signal-to-noise ratio of all six rats before and after modification, p=.0008. (e) is the heat map of SNR results for each rat at each stimulate frequency.

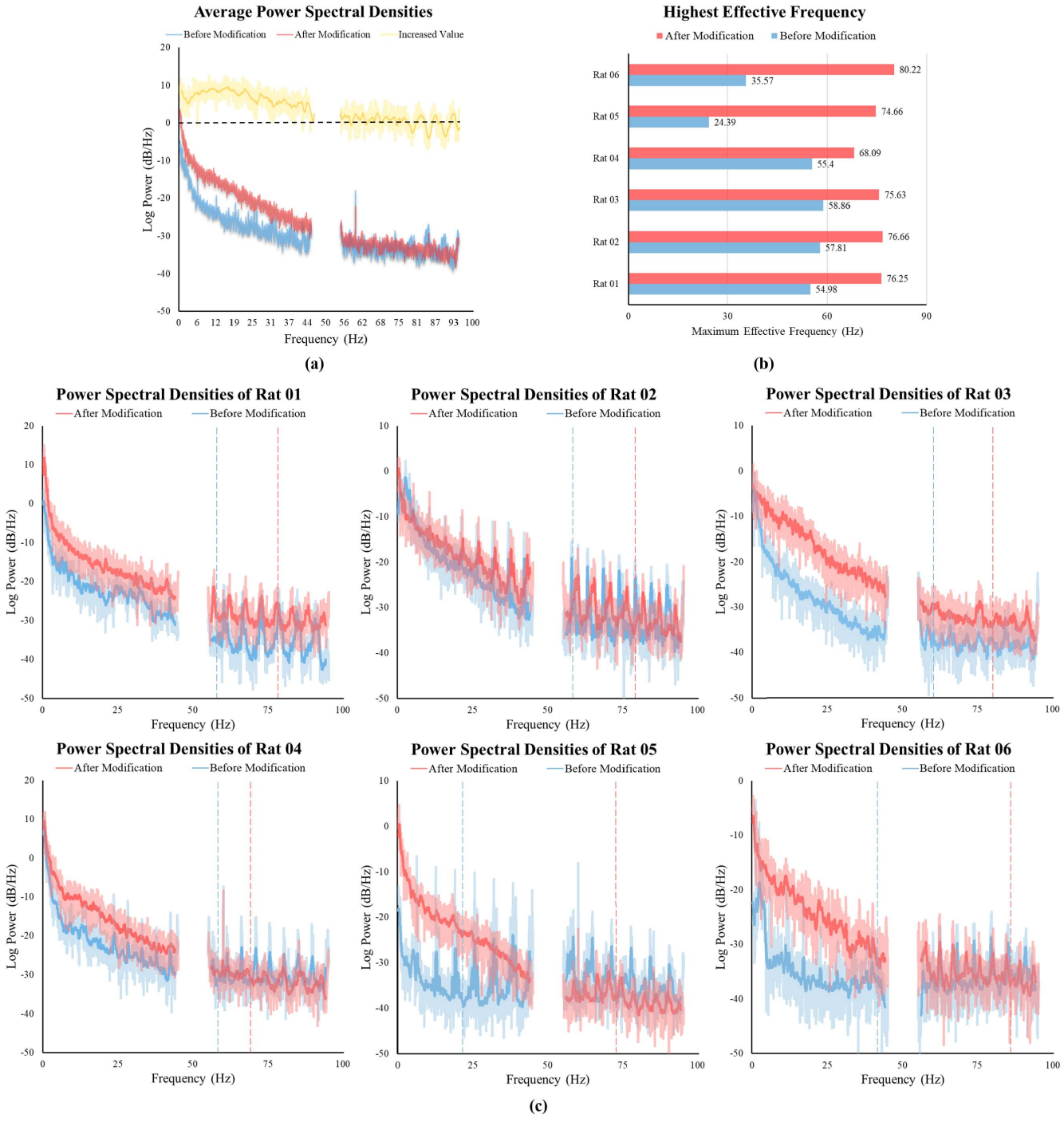

Fig. 6. Power spectral densities of rats' rsEEG before and after MILEM. (a) shows the average PSD of all rats before and after MILEM. The yellow part is increased value by MILEM, MEAN=3.79 dB, SD=3.93. The interference of the 60Hz frequency component comes from the operating frequency of the stimulation screen.

the modification scheme has far more potential in exploring electrophysiological meanings via different modalities of pericephalic approach. Since the skull bone is similarly a barrier to optical and acoustic signals, MILEM scheme presented in this paper would also open the door for light and sound propagation and hence elevate the quality of signal attained. While the specific boosting effect needs to be further specified in later studies, there is no denying that the potential improvement of this scheme on functional near-infrared spectroscopy (fNIRS) and functional ultrasound neuroimaging (fUS) is very promising.

D. Working Temperature of Piezoelectric Drill

The inability of the hole healing after MILEM caught our attention. There may be many reasons for this, but we

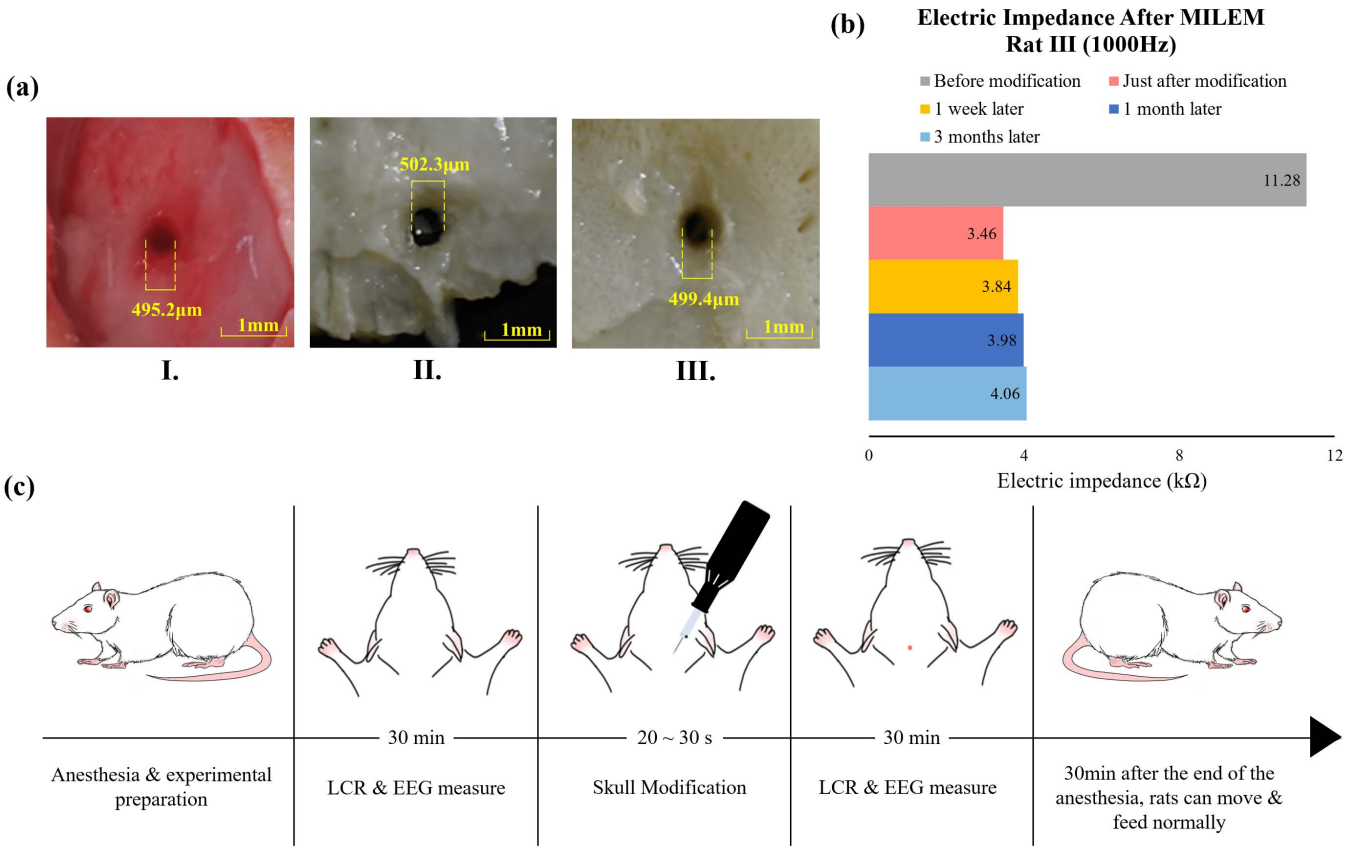

Fig. 7. (a) Skull holes captured by micro-lens. Of which I. was taken promptly after modification. II. A photograph was taken one week after the modification. III. A photograph was taken three months after the modification. (b) is the bar graph of the electrical impedance results recorded by LCR bridge at different times after MILEM at 1000Hz measurement frequency. (c) shows the timeline of the whole experiment protocol including MILEM procedure. Rats return to normal life as soon as awaking from anesthesia, indicating the harmlessness of MILEM.

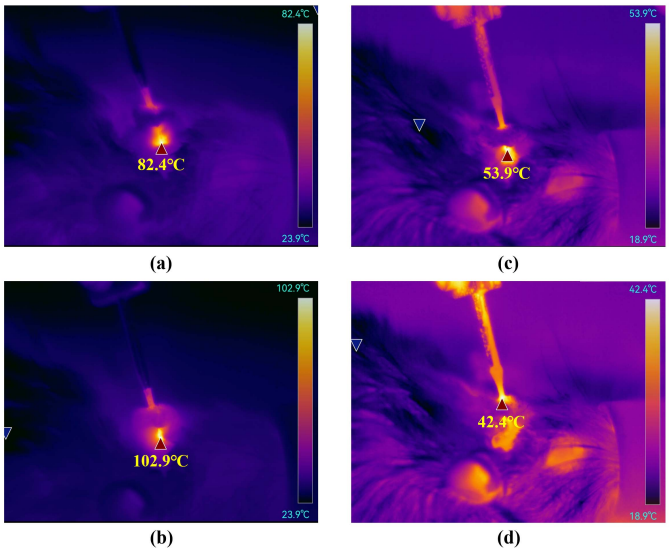

Fig. 8. Infrared images of MILEM. (a) after 20 s of work without cooling measures. (b) after 40 s of work without cooling measures. (c) 20 s of work under cooling measures. (d) 40 s of work while cooling measures were taken.

speculate that the most predominant reason is the local high temperature that piezoelectric drills produce while working. We subsequently measured the working temperature at the time of skull reformation using infrared detection equipment to gain information for explanation. For ease of observation, the right scalp of the rat had been removed prior to modification.

Figure 8 shows the experimental results, where (a) the infrared image after 20 seconds without cooling measures shows that the contact temperature has reached 82.4 °C. (b) is the infrared image after 40 s in the case of not taking cooling measures, the contact temperature has reached 102.9 °C. (c) and (d) is the infrared images after working for 20 s and 40 s under the condition of taking cooling measures. It can be seen that the working temperature can be stabilized at about 50 °C. However, since the liquid used for cooling will block infrared emission, we believe that even in the case of taking cooling measures, drill bit and bone tissue interface temperature is likely to be above 80 °C. This local temperature is suffice to inactivate the contact surface tissue, thereby causing it to lose healing capability. Nevertheless, the specific reasons still need further investigation.

V. Conclusion

Throughout the history of non-invasive BCI development, huge progress has been made on innovative applications in early decades. However, looking back at the current situation, research in this field seems to stagnate due to its upper limit

of signal quality for that the accuracy and precision fail to outperform ECoG. However, EEG has this huge non-invasive advantage over ECoG that is not easy to be replaced. Hence to address this issue, we proposed a low surgical risk technical scheme for minimally invasive local skull electrophysiological modification using a piezoelectric surgical drill. It can improve the signal quality recorded by EEG by breaking through the signal barrier—the skull without damaging any soft tissue below.

To testify the feasibility of the scheme, rats were used as animal models for in vivo verification experiments. Six 8-month-old SD rats were used, including three males and three females. A special designed piezoelectric surgical drill, the bit of which was coated with a layer of silicon carbide, was used to open a hole with a diameter of about 500 micrometers without removing any skin in the skull above the visual area of rats. The electrical impedance values at different frequencies from the ear to the modification point before and after the transformation are recorded by LCR digital bridge. Meanwhile, the EEG signals under SSVEP stimulation and rsEEG signals were recorded. The electrical impedance value has decreased by about 84 %, the SSVEP signal broadband SNR has increased by about 5.13 dB, and the highest effective frequency of EEG signal in the resting state has increased by about 57 %. The survival rate of six rats after three months was 100 %, and no obvious infection symptoms were observed. At the same time, there was no apparent tendency of holes healing left by skull modification.

Overall, the technical scheme of minimally invasive local skull electrophysiological modification presented in this article is proved to be practicable. Its contribution to the EEG signal elevation and the electrical impedance reduction is significant while it also ensures almost no surgical risks. Thus it is suffice to say that MILEM possesses great capacity in enhancing EEG signal quality to ECoG level and even exceed and replace it for its higher safety in clinic applications in future.

Acknowledgment

The authors would like to thank Yixin Zhang for her help in animal experiments and Prof. Bai Lu for providing experimental materials.

References

[1] X. Chen *et al.*, "Filter bank canonical correlation analysis for implementing a high-speed SSVEP-based brain–computer interface," *J. Neural Eng.*, vol. 12, no. 4, 2015, Art. no. 046008.

[2] X. Chen *et al.*, "High-speed spelling with a noninvasive brain–computer interface," *Proc. Nat. Acad. Sci. USA*, vol. 112, no. 44, pp. E6058–E6067, 2015, doi: 10.1073/pnas.1508080112.

[3] C. Pandarinath *et al.*, "High performance communication by people with paralysis using an intracortical brain–computer interface," *eLife*, vol. 6, Feb. 2017, Art. no. e18554, doi: 10.7554/elife.18554.

[4] F. R. Willett, D. T. Avansino, L. R. Hochberg, J. M. Henderson, and K. V. Shenoy, "High-performance brain-to-text communication via handwriting," *Nature*, vol. 593, no. 7858, pp. 249–254, May 2021, doi: 10.1038/s41586-021-03506-2.

[5] X. Gao *et al.*, "Interface, interaction, and intelligence in generalized brain–computer interfaces," *Trends Cogn. Sci.*, vol. 25, no. 8, pp. 671–684, 2021.

[6] G. Grübler *et al.*, "Psychosocial and ethical aspects in non-invasive EEG-based BCI research—A survey among BCI users and BCI professionals," *Neuroethics*, vol. 7, no. 1, pp. 29–41, 2014, doi: 10.1007/s12152-013-9179-7.

[7] B. Allison, T. Lüth, D. Valbuena, A. Teymourian, I. Volosyak, and A. Gräser, "BCI demographics: How many (and what kinds of) people can use an SSVEP BCI?" *IEEE Trans. Neural Syst. Rehabil. Eng.*, vol. 18, no. 2, pp. 107–116, Apr. 2010,doi: 10.1109/TNSRE.2009.2039495.

[8] C. Guger *et al.*, "How many people are able to control a P300-based brain–computer interface (BCI)?" *Neurosci. Lett.*, vol. 462, no. 1, pp. 94–98, Oct. 2009.

[9] J. E. Huggins, *BCIs Based on Signals From Between the Brain and Skull*. Berlin, Germany: Springer, 2009, pp. 221–239.

[10] B. Wittevrongel *et al.*, "Decoding steady-state visual evoked potentials from electrocorticography," *Frontiers Neuroinform.*, vol. 12, p. 65, Sep. 2018, doi: 10.3389/fninf.2018.00065.

[11] E. Klein, "Informed consent in implantable BCI research: Identifying risks and exploring meaning," *Sci. Eng. Ethics*, vol. 22, no. 5, pp. 1299–1317, Oct. 2016, doi: 10.1007/s11948-015-9712-7.

[12] I. S. Kourbeti *et al.*, "Infections in patients undergoing craniotomy: Risk factors associated with post-craniotomy meningitis," *J. Neurosurg.*, vol. 122, no. 5, pp. 1113–1119, May 2015, doi: 10.3171/2014.8.jns132557.

[13] A. D. Maynard and M. Scragg, "The ethical and responsible development and application of advanced brain machine interfaces," *J. Med. Internet Res.*, vol. 21, no. 10, Oct. 2019, Art. no. e16321, doi: 10.2196/16321.

[14] B. Z. Allison *et al.*, "Brain–computer interface systems: Progress and prospects," *Expert Rev. Med. devices*, vol. 4, no. 4, pp. 463–474, 2007, doi: 10.1586/17434440.4.4.463.

[15] J. A. Malmivuo and V. E. Suihko, "Effect of skull resistivity on the spatial resolutions of EEG and MEG," *IEEE Trans. Biomed. Eng.*, vol. 51, no. 7, pp. 1276–1280, Jul. 2004, doi: 10.1109/TBME.2004.827255.

[16] S. Rush and D. A. Driscoll, "Current distribution in the brain from surface electrodes," *Anesthesia Analgesia*, vol. 47, no. 6, pp. 717–723, 1968.

[17] S. Rush and D. A. Driscoll, "EEG electrode sensitivity—An application of reciprocity," *IEEE Trans. Biomed. Eng.*, vol. BME-16, no. 1, pp. 15–22, Jan. 1969.

[18] T. F. Oostendorp, J. Delbeke, and D. F. Stegeman, "The conductivity of the human skull: Results of *in vivo* and *in vitro* measurements," *IEEE Trans. Biomed. Eng.*, vol. 47, no. 11, pp. 1487–1492, Nov. 2000, doi: 10.1109/TBME.2000.880100.

[19] Y. Lai *et al.*, "Estimation of *in vivo* human brain-to-skull conductivity ratio from simultaneous extra-and intra-cranial electrical potential recordings," *Clin. Neurophysiol.*, vol. 116, no. 2, pp. 456–465, 2005.

[20] K. M. Van De Graaff, *Human Anatomy* (Engineering & Mathematics), no. 2. New York, NY, USA: McGraw-Hill, 1911.

[21] G. Huiskamp, M. Vroeijenstijn, R. van Dijk, G. Wieneke, and A. C. van Huffelen, "The need for correct realistic geometry in the inverse EEG problem," *IEEE Trans. Biomed. Eng.*, vol. 46, no. 11, pp. 1281–1287, Nov. 1999, doi: 10.1109/10.797987.

[22] R. Oostenveld and T. F. Oostendorp, "Validating the boundary element method for forward and inverse EEG computations in the presence of a hole in the skull," *Hum. Brain Mapping*, vol. 17, no. 3, pp. 179–192, Nov. 2002, doi: 10.1002/hbm.10061.

[23] L. Flemming, Y. Wang, A. Caprihan, M. Eiselt, J. Haueisen, and Y. Okada, "Evaluation of the distortion of EEG signals caused by a hole in the skull mimicking the fontanel in the skull of human neonates," *Clin. Neurophysiol.*, vol. 116, no. 5, pp. 1141–1152, May 2005.

[24] S. Lau, L. Flemming, and J. Haueisen, "Magnetoencephalography signals are influenced by skull defects," *Clin. Neurophysiol.*, vol. 125, no. 8, pp. 1653–1662, Aug. 2014.

[25] K. Kendel and H. Koufen, "EEG-Veränderungen bei cerebralen Gefäßinsulten des Hirnstamms," *Deutsche Zeitschrift für Nervenheilkunde*, vol. 197, no. 1, pp. 42–55, 1970, doi: 10.1007/bf00242249.

[26] W. A. Cobb, R. J. Guiloff, and J. Cast, "Breach rhythm: The EEG related to skull defects," *Electroencephalogr. Clin. Neurophysiol.*, vol. 47, no. 3, pp. 251–271, Sep. 1979.

[27] X. Chen, Z. Chen, S. Gao, and X. Gao, "A high-ITR SSVEP-based BCI speller," *Brain-Comput. Interfaces*, vol. 1, nos. 3–4, pp. 181–191, 2014.

[28] M. Hamedi, S. H. Salleh, and A. M. Noor, "Electroencephalographic motor imagery brain connectivity analysis for BCI: A review," *Neural Comput.*, vol. 28, no. 6, pp. 999–1041, Jun. 2016.
[29] J. Mak *et al.*, "Optimizing the P300-based brain–computer interface: Current status, limitations and future directions," *J. Neural Eng.*, vol. 8, no. 2, 2011, Art. no. 025003.
[30] H. Machemer, "Electrophysiology," in *Paramecium*. Berlin, Germany: Springer 1998, pp. 185–215, doi: 10.1007/978-3-642-73086-3_13.
[31] G. Pavlíková, R. Foltán, M. Horká, T. Hanzelka, H. Borunská, and J. Šedý, "Piezosurgery in oral and maxillofacial surgery," *Int. J. Oral Maxillofacial Surg.*, vol. 40, no. 5, pp. 451–457, May 2011.
[32] S. Stübinger, J. Kuttenberger, A. Filippi, R. Sader, and H.-F. Zeilhofer, "Intraoral piezosurgery: Preliminary results of a new technique," *J. Oral Maxillofacial Surg.*, vol. 63, no. 9, pp. 1283–1287, Sep. 2005.
[33] M. Rahnama *et al.*, "The use of piezosurgery as an alternative method of minimally invasive surgery in the authors' experience," *Videosurg. Other Miniinvasive Techn.*, vol. 8, no. 4, p. 321, 2013.
[34] M. Schlee, M. Steigmann, E. Bratu, and A. K. Garg, "Piezosurgery: Basics and possibilities," *Implant Dentistry*, vol. 15, no. 4, pp. 334–340, 2006.
[35] B. Kotrikova *et al.*, "Piezosurgery—A new safe technique in cranial osteoplasty?" *Int. J. Oral Maxillofacial Surg.*, vol. 35, no. 5, pp. 461–465, 2006.
[36] U. Salem *et al.*, "Neurosurgical applications of MRI guided laser interstitial thermal therapy (LITT)," *Cancer Imag.*, vol. 19, no. 1, Dec. 2019, doi: 10.1186/s40644-019-0250-4.
[37] N. Galloway, "Human brain electrophysiology: Evoked potentials and evoked magnetic fields in science and medicine," *Brit. J. Ophthalmol.*, vol. 74, no. 4, p. 255, 1990.
[38] P. Xu *et al.*, "Cortical network properties revealed by SSVEP in anesthetized rats," *Sci. Rep.*, vol. 3, no. 1, Dec. 2013, doi: 10.1038/srep02496.
[39] A. Bondar and L. Shubina, "Nonlinear reactions of limbic structure electrical activity in response to rhythmical photostimulation in Guinea pigs," *Brain Res. Bull.*, vol. 143, pp. 73–82, Oct. 2018.
[40] Y. Wang, X. Gao, B. Hong, C. Jia, and S. Gao, "Brain–computer interfaces based on visual evoked potentials," *IEEE Eng. Med. Biol. Mag.*, vol. 27, no. 5, pp. 64–71, Sep. 2008.
[41] J. C. Christensen, J. R. Estepp, G. F. Wilson, and C. A. Russell, "The effects of day-to-day variability of physiological data on operator functional state classification," *NeuroImage*, vol. 59, no. 1, pp. 57–63, Jan. 2012.
[42] D. H. Brainard, "The psychophysics toolbox," *Spatial Vis.*, vol. 10, no. 4, pp. 433–436, 1997.
[43] J. Thielen *et al.*, "Broad-band visually evoked potentials: Re (con) volution in brain–computer interfacing," *PloS ONE*, vol. 10, no. 7, 2015, Art. no. e0133797.
[44] E. Niedermeyer and F. L. da Silva, *Electroencephalography: Basic Principles, Clinical Applications, and Related Fields*. Philadelphia, PA, USA: Lippincott Williams & Wilkins, 2005.
[45] D. T. Bundy *et al.*, "Characterization of the effects of the human dura on macro-and micro-electrocorticographic recordings," *J. Neural Eng.*, vol. 11, no. 1, 2014, Art. no. 016006.
[46] T. J. Oxley *et al.*, "Minimally invasive endovascular stent-electrode array for high-fidelity, chronic recordings of cortical neural activity," *Nature Biotechnol.*, vol. 34, no. 3, pp. 320–327, 2016, doi: 10.1038/nbt.3428.
[47] Y. Wang, X. Chen, X. Gao, and S. Gao, "A benchmark dataset for SSVEP-based brain–computer interfaces," *IEEE Trans. Neural Syst. Rehabil. Eng.* vol. 25, no. 10, pp. 1746–1752, Nov. 2016, doi: 10.1109/TNSRE.2016.2627556.